Finite Element Analysis of Endodontically Treated Teeth with Simulated Variable Bone Level Restored with Two Types of Prefabricated Posts

Hoda Elazhary, Eman Anwar, Ahmed El Ragy, and Amany Ramadan

Abstract—The present study was carried out to compare between Ti post and Glass fiber reinforced composite post on stress distribution in endodontically treated maxillary central incisors with variable bone support. Computational 3-D FEA method was used to determine the stresses created in specimens. For both tested posts with decreased simulated bone support concentration of tension stresses increased in root, post and bone but decreased in core and crown. For both post types stresses are more concentrated apically but with less stress values created in case of the tested fiber post thus decreasing the risk for root fracture.

Index Terms— Bone level, Central incisor, Displacement, Finite Element Analysis, Fiber Post, Stress Analysis, Titanium Post.

1 INTRODUCTION

DURING clinical practice, restoration of endodontically treated teeth is almost encountered daily. Most of these teeth require using a post-core system for retention of coronal restoration to compensate for the excessive structural loss [1]. This technique offers the possibility of restoring mutilated teeth without requiring aggressive procedures [2].

Although metal posts have been used for years, studies have questioned their performance regarding aesthetics, biocompatibility, retention and stress distribution [3]. With the increased aesthetic demands, tooth colored post and core systems were introduced in the market since the late 80`s [4-5].

Several studies were conducted to aid in the determination of the best post-core system to be used in different clinical situations. Some of these studies [6-12] used experimental testing of prepared specimens. Others [13-18] used the computational finite element analysis method.

The prominent approach in practice is conservatism avoiding teeth extraction, whenever possible, aided by the proved efficacy of long term periodontal maintenance. This lead to realizing the importance of using post-core systems for teeth with variable loss of bone support [15]. The research studies concerned with the type of post and core system to be used shows great controversy [13]. This implies that there is still much work to be done in this area of research.

Consequently, this research study is concerned with evaluating the effect of two different ready-made posts on the stress distribution of endodontically treated teeth with simulated variable bone support using numerical testing (Finite Element Analysis FEA). The paper is organized as follows: Section 2 presents the preparation phase and testing phase in case of numerical testing. The results are demonstrated in Section 3. Finally, Section 4 presents the discussions and conclusions.

2 NUMERICAL TESTING

Finite element analysis is a numerical tool used for simulation of different models involving various structures. It can be used to establish a direct relation between forces and displacement. Thus, it allows for simulation of behavior of structure even those with complex geometries via providing detailed mechanical responses. This process is carried out in three main steps; preprocessing, processing and post processing.

2.1 Preprocessing

In simulation of the actual cases, a 3-D model of a post-core-crown restored human endodontically treated maxillary central incisor with its investing structure was constructed using a three step procedure;

- Multislice Computed Tomographic (CT) scanning.
- Use of Materialise's Interactive Medical Image Control System (MIMICS).
- Modeling of the rehabilitation system with the investing structure.

2.1.1 Computed Tomographic Scanning CT:

An accurate model with the actual shape and geometric dimensions of a human central incisor, was created. An average sized recently extracted defect free maxillary central incisor was cleaned using an ultrasonic scaller and stored in 0.9% saline. Computerized tomography (CT) was carried out at the Radiology Department, Military production Specialized Medical Center (Helwan), using multislice CT (MSCT GE medical system with a dedicated dental software). The scanning parameters are listed in Table (1).

- *Hoda H. Elazhary is currently pursuing masters degree program in fixed Prothodontics in Cairo University and an assistant researcher at the National Research Center, Cairo, Egypt. E-mail: hodas79@hotmail.com*
- *Dr. Eman Mohamed Anwar, Professor of Fixed Prosthodontics, Faculty of Oral and Dental Medicine, Cairo University.*
- *Dr Ahmed Fouad El Ragy, Lecturer in Civil Engineering Department, Faculty of Engineering, Fayoum University*
- *Dr. Amany Ramadan, Researcher in Oral and Dental Medicine Research Division, National Research Center.*

Table (1) Representing a summary of the scan parameters:

Slice Thickness	0.625 mm
Table speed	0.5mm/0.5s
Reconstruction interval	0.5mm
KVp	120
MAm	140
Field of view	20.3 cm
Matrix	512x512

Use of Materialise's Interactive Medical Image Control System (MIMICS):

It is using an interactive tool for visualization and segmentation of CT and MRI images. In addition, it aids in 3D rendering of objects. It can process any number of 2D image slices and render them into 3D images. In this study, the Materialise's Interactive Medical Image Control System (MIMICS) was used to generate a 3D model of an upper central incisor tooth and to optimize the model for other processor software, ANSYS for finite element analysis (FEA). By using the FEA/CFD module in MIMICS, triangulation of the surface (STL- Standard Triangulation Language) can be modified and a better mesh can be achieved. The 3D objects were then exported into Ansys software for further analysis.

Steps followed in MIMICS were as follows:

Importing images:

The entire process starts by importing images from a scanned system and converting it into a MIMICS project file (.mcs); MIMICS imports computed tomography (CT) and magnetic resonance imaging (MRI) data in a wide variety of formats and allows for extended visualization and segmentation functions based on image density thresholding.

Segmentation and Thresholding:

The first step of segmentation is the threshold step, where the structures of interest are selected based on the gray values (Hounsfield Units (HU)). Thresholding means that the segmentation object (visualized by a colored mask) will contain only those pixels of the image with a value higher than or equal to the threshold value. Sometimes an upper and lower threshold is required; the segmentation mask contains all pixels between these two values. By setting the threshold value at a certain range, a mask for the region of interest can be selected. For the case under study, the region of interest is the central incisor. A mask that contains all the pixels in that particular range is created.

3D generation

3D object is automatically created in the form of masks by growing a threshold region on the entire stack of scans.

Remeshing

Native STLs are improper for use in finite element analysis (FEA) because of the aspect ratio and connectivity of the triangles in these files. The REMESH module attached to MIMICS was therefore used to automatically reduce the amount of triangles and simultaneously improve the quality of the triangles while maintaining the geometry. During remesh, the tolerance variation from the original data can be specified. The quality is defined as a measure of triangle height/base ratio so that the file can be imported in the finite element analysis (FEA) software package without generating any problem.

2.1.2 Modeling of the rehabilitation system with the investing structure:

In the present study both ParaPost fiber Lux and ParaPost XH (Coltene whaledent Inc. Cuyahoga falls USA) were used. The dimensions of the post size used were 14 mm length and 1.5 mm diameter. Using Ansys 11 the post , the investing and rehabilitation structures were created to coincide with actual condition; periodontal ligament, bone, endodontic filling, post, luting cement, core and crown.

Points indicating every layer are called key points that are connected together producing volumes. These volumes are then assembled like building blocks to approximate the whole model in return. Thus the process is "a finite element approximation of a structure". The model was cut into smaller volumes called elements for more accurate results by assigning the loads to finer sizes. These elements are connected at the corner points by nodes. This is called meshing "finite element mesh". This is either done by choosing the size of the small volumes or by determining the number to which every line in the structure is to be divided into. In this study the mesh size was determined by dividing every line into smaller 6 segments.

Element Type

The used element type is (SOLID95 3-D 20- Node Structural Solid). It can tolerate irregular shapes without much loss of accuracy. Its elements have compatible displacement shapes and are well suited to model curved boundaries.

Every element is defined by 20 nodes having three degrees of freedom per node i.e. translations in the nodal X, Y and Z directions. The element may have any spatial orientation. The element has plasticity, creep stress stiffening, large deflection, and large strain capabilities. Various printout options are also available. Number of elements and nodes in the present study for different models are listed in Table (2).

Table (2): Number of elements and nodes for different models:

Model	Elements	Nodes
2mm	23.551	141.748
2.5mm	24.634	135.224
3mm	25.767	128.359

Material Property

All materials used in the present study were considered to be isotropic, homogeneous, and linearly elastic. Only two material properties are required for linear elastic Finite Element Analysis (FEA; Elastic modulus (E) and Poisson's ratio. Material properties were specified to the coinciding appropriate elements in Table (3).

Although published elastic properties for dentin and enamel show some variability; they are much more definitively characterized. Single values of Young's modulus and Poisson's ratio for dentin and enamel were chosen from the literature.

Table (3): Modulus of elasticity and Poisson's ratio for elements involved in the present study:

Material	Modulus of elasticity (MPa)	Poisson's ratio	References
Dentine	18.6×10^9	0.31	(13-15, 19-22 33)
Enamel	41×10^9	0.30	(13, 19, 23, 24)
Cementum	2.398×10^9	0.31	(19)
Periodontal ligament	0.0689×10^9	0.45	(24, 19)
Alveolar bone	13.8×10^9	0.26	(14)
Composite resin core	10×10^9	0.24	(27)
Glass ionomer cement	22×10^9	0.35	(17)
Metal coping (NiCr)	205×10^9	0.33	(15,17)
Titanium alloy post	117×10^9	0.33	(14, 19)
Fiber reinforced composite post	45×10^9	0.32	(13-15, 26, 28)
Gutta percha	0.00069×10^9	0.45	(13,14,20 ,23)
Quixfil	12×10^9	0.35	(20)
RelayX unicem	7×10^9	0.30	(13,15,20,21-23, 29)

Load

The applied load is 100 N at 45° at the junction between the incisal and the middle thirds of the lingual surface of the tooth crown.

Support/boundary condition

It represents the operating condition for the design and how it is tied to the ground. The applied support was on the bone outer surface thus preventing displacement in the X, Y and Z directions.

All pre and post processing steps were carried out under Microsoft Window Vista by Intel Core 2 processor with 1 GB ram computer.

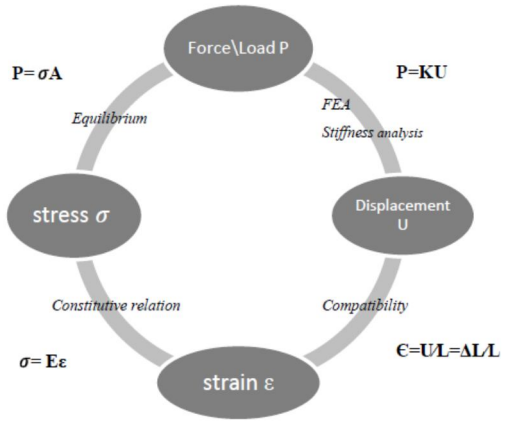

2.2 Processing

After the finite element modeling; creation and meshing of the design, applying material properties, loads and boundaries, the mathematical analysis could be executed. It consists of characterizing the displacement behavior of an element under a set of prescribed loads. The analysis is formulated as a matrix algebra resulting in a system of simultaneous equations representing the relation between both the loads and the displacement. These equations, mostly being huge in number could only be solved using a computer. Thus, any development in the finite element method is closely related to the development in the computers. The accuracy of the results is highly dependent on the accuracy of the element modeling.

The mathematical formula is as follows;

P = K U

Where,

P = Load vector

K = Overall stiffness matrix (material property and geometry)

U = Displacement vector

Є =Young modulus

In the previous diagram, it is clarified that the FEA acts as a short cut between load and displacement.

2.3 Post processing

2.3.1 Using ANSYS general postprocessor contour color plots of the maximum and minimum first (S1) and third (S2) principle stresses together with the von misses stresses, were created and analyzed in dentine.

Von misses stress

The Von Misses is a formula for combining the 3 dimensional systems of stresses, created at any point within a 3 dimensional elastic body when subjected to a system of loads in 3dimensions, into an equivalent stress. It refers to a theory called the "Von Misses - Hencky criterion for ductile failure". The Von Misses criterion is a formula for calculating whether the stress combination at a given point will cause failure; even though none of the principal stresses exceeds the yield stress of the material, it is possible for yielding to result from the combination of stresses, which is then compared to the yield stress of the material. If the "Von Mises Stress" exceeds the yield stress, then the material is considered at risk of failure.

The formula is

(S1-S2) 2 + (S2-S3) 2 + (S3-S1) 2 = 2Se2

Where S1, S2 and S3 are the principal stresses and Se is the equivalent stress, or "Von Mises Stress".

The effect of change in bone height; 2, 2.5 and 3mm apical to C.E.J., with the use of different post material; titanium and FRC, were studied and analyzed.

3 Results

In the present study a theoretical finite element analysis was carried out. The results were analyzed thus reaching a conclusion.

3.1 Results of the theoretical 3D Finite Element Analysis method (FEA):

3.1.1 Stress analysis:

The load applied to the simulated restored post-core-crown complex was 100 N applied to the palatal surface with a 45° angle at the junction of the incisal and middle thirds. This direction induced a tendency of post flexion in a labial direction. As a result, compressive stresses were induced in the tested structures labially while tension stresses were induced palataly.

In the present study the effect of two different posts together with the variation in bone support were presented. All contour color plot analysis were established for all studied cases. For all models considered, the maximum tensile stresses (maximum first principle stress) (S1), the maximum compressive stresses (maximum third principle stress) (S3) and the whole stress field (von misses stress) (Seqv) were determined. All stresses were determined in Mega Pascal`s (MPa) and summarized.

When analyzing the tested models, they were named according to post type and bone level; 1A, 1B, 1C, 2A, 2B, 2C. The number 1 refers to to the fiber post, while the number 2 refers to the titanium post. The letters used; A, b, C referred to the bone level from the assumed cemento enamel junction under investigation.

All tested models were disassembled to identify stresses occurring upon load application in every structure separately. The components of the FE models that were analyzed are; the bone, the root, the post, the crown and the core. Stress distribution is represented with a contour color scale where warmer colors (red orange and yellow) represent the higher values while the cooler colors (blue and green) represent the lower values and vice versa for compressive stresses only. The highest value for every model was determined and compared.

- **Tensile stress distribution patterns (Maximum first principle stress) (Maximum tensile stress) (S1) (Table 4)**

Table 4: S_1 (maximum tensile stress) in Mega Pascal's (MPa) of all components of tested samples at different tested conditions:

Specimen \ Structure	Bone	Root	Post	Crown	Core
2A *Titanium post +2mm bone level*	133.153	92.055	28.837	119.543	3.774
2B *Titanium post +2.5mm bone level*	139.079	108.54	31.208	118.997	3.878
2C *Titanium post +2mm bone level*	219.027	149.987	36.963	117.093	4.097
1A *FRC post +2mm bone level*	133.142	90.908	10.257	121.72	3.312
1B *FRC post +2.5mm bone level*	139.756	107.296	10.963	121.27	3.314
1C *FRC post +3mm bone level*	218.37	148.631	13.161	119.612	3.312

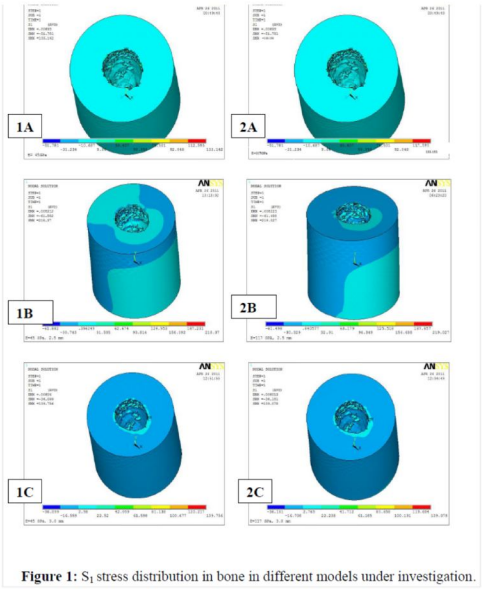

Figure 1: S_1 stress distribution in bone in different models under investigation.

Analyzing contour color plot analysis of the maximum first principle stress in bone in all tested models, it was found that the highest value of S1 was found in model (2C) followed by model (1C) then by model (1B) and model (2B) with almost no difference between them. Model (2A) and (1A) came fourth and fifth respectively. The distribution of S1 stress did not vary between models. The highest value of S1 was found cervically on the inner aspect of bone in all models. The S1 stress distribution was almost uniform throughout the whole bone structure and was higher in (2) models when compared to their likewise in (1) models. Values of S1 in bone are found to increase by decrease in bone level as shown in Figure 1.

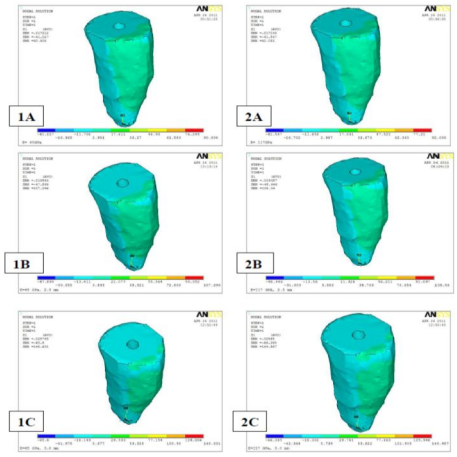

Figure 2: S_1 stress distribution in root in different models under investigation.

In root, contour color plot analysis of the maximum first principle stress showed that the highest S1 value was found in model (2C) followed by (1C), (2B), (1B),(2A), and (1A) respectively. The distribution of S1 stress is found to be quite similar in all models with minimum concentration at the apical third. Values of S1 in root is inversely proportional to bone level and are higher in (2) models when compared to their likewise in (1) models as shown in Figure 2.

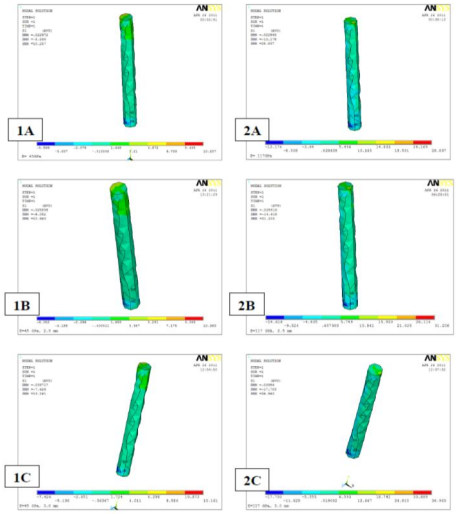

Figure 3: S_1 stress distribution in post in different models under investigation.

Regarding S1 stresses created in the post, contour color plot analysis of the maximum first principle stress showed that the models with titanium post (2) showed higher values than the models with fiber reinforced composite post (1) in the following order (2C), (2B), (2A), (1C), (1B), (1A) respectively. Regarding the S1 stress distribution, the common between all models is that the maximum S1 was found apically and the area of the minimum value was found right cervical to it. The distribution of stresses along the body of the post was better in (1) models.

Although both the (1) and (2) models showed some sort of stress concentration incisally but still in the (1) models it was distributed over a larger area when compared to its likewise in (2) models. Considering the values of S1 in bone, they increased by decrease in bone level and where higher in (2) models when compared to their likewise in (1) model as shown in Figure 3.

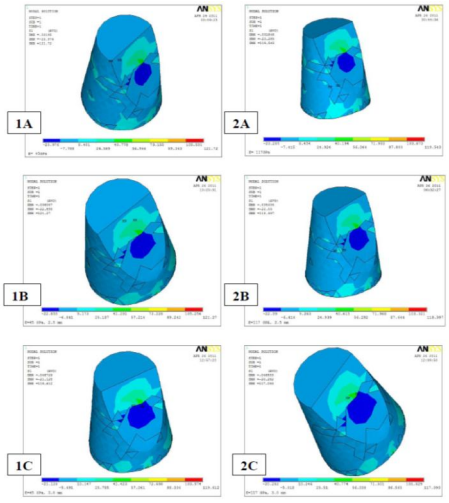

Figure 4: S_1 stress distribution in crown in different models under investigation.

On the other hand, when considering the S1 stresses created in the crown of all tested models, the (1) group came first as follows (1A), (1B), (1C), (2A), (2B), (2C) respectively. Contour color plot analysis of the maximum first principle stress showed that stress distribution in all models was almost similar with max stress concentration cervically and at point of load application with area of minimum stress concentration just cervical to it.

Surprisingly the values of the S1 stress in crown were directly proportional to bone level and were higher in the (1) models than in the (2) models as shown in Table 4 and Figure 4.

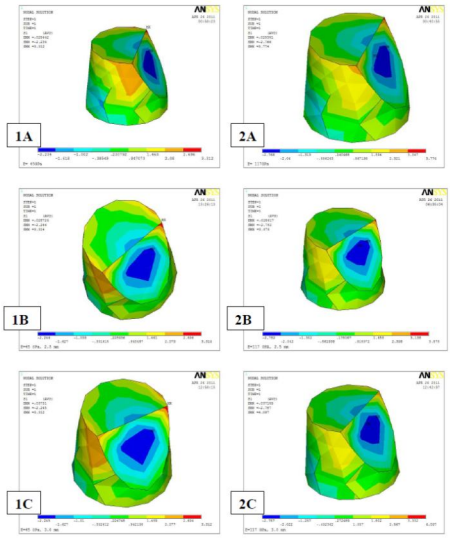

Figure 5: S_1 stress distribution in core in different models under investigation.

Composite resin core S1 stresses were highest in model (2C) followed by model (2B). In third place came model (2A) followed by all (1) models that showed almost no difference in between. Regarding stress distribution using contour color plot analysis of the maximum first principle stress in core showed that in both (1) and (2) models the maximum stress concentration was at the incisal line angles of the core. In the (1) models another area of S1 stress concentration existed at the proximal walls incisally. Minimum S1 stresses existed at the lingual aspect of the core as shown in Figure 5.

When considering the S3 stress in tested models, the highest value was found in bone in model (1C) followed by model (2C), (1B), (2B), (1A) and (2A) respectively. Contour color plot analysis of the maximum third principle stress in bone of all tested models showed that stress distribution in both (2) and (1) models was comparable at every bone level.

- **Compressive stress distribution patterns (Maximum third principle stress) (Maximum compressive stress) (S3) (Table 5)**

Table 5: S_3 (maximum compressive stress) in Mega Pascal`s (MPa) of the components of tested samples at different tested conditions:

Structure / Specimen	Bone	Root	Post	Crown	Core
2A *Titanium post +2mm bone level*	161.728	71.516	25.321	88.303	12.002
2B *Titanium post +2.5mm bone level*	188.605	84.412	25.865	86.246	12.218
2C *Titanium post +3mm bone level*	194.737	116.75	31.64	85.694	12.503
1A *FRC post +2mm bone level*	162.872	70.582	18.386	88.736	10.188
1B *FRC post +2.5mm bone level*	189.412	83.395	18.251	88.314	10.295
1C *FRC post +3mm bone level*	195.478	115.634	18.455	85.365	10.427

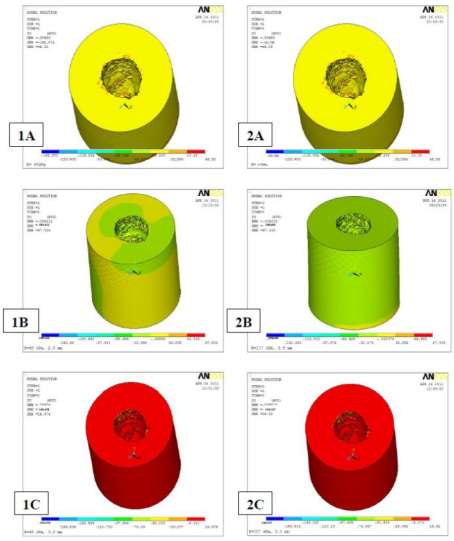

Figure 6: S_3 stress distribution in bone in different models under investigation.

At both 2mm and 2.5mm bone levels stresses were mainly concentrated along the root side of the bone. At 3mm bone level stresses were concentrated both at the inner and outer aspects of the bone. Although the S3 values in bone in (1) models were higher than their likewise in (2) models, the difference was not significant. S3 stress in bone increased by decrease in bone level as shown in Figure 6.

In roots of all tested models, S3 stress was found highest in model (2C) followed by model (1C), (2B), (1B), (2A) and (1A) respectively. Contour color plot analysis of the maximum third principle stress in root of all tested models showed that stress distribution in both (2) and (1) models was almost the same with minimum stresses created apically. Although values in (2) models were higher than their likewise in (1) models, the difference was not significant. S3 stress in root increased by decrease in bone level as shown in Figure 7.

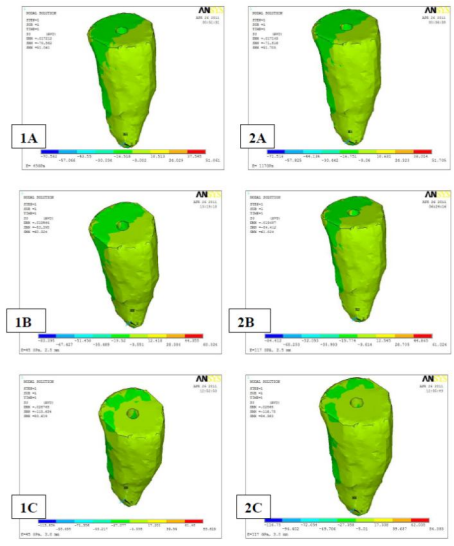

Figure 7: S_3 stress distribution in root in different models under investigation.

S3 stress distribution in post in different models under investigation is represented and the values listed in a descending order are as follows; (2C), (2B), (2A), (1C), (1B), and (1A).

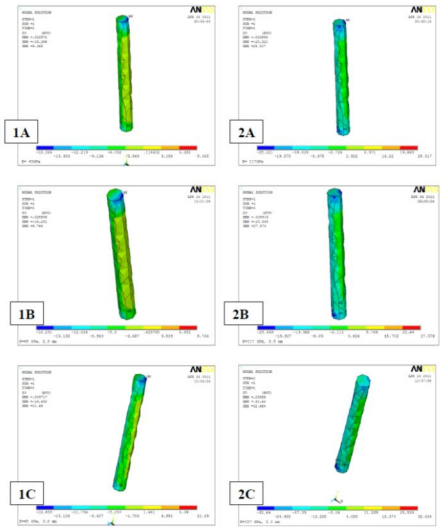

Figure 8 : S_3 stress distribution in post in different models under investigation.

Contour color plot analysis of the maximum third principle stress showed that stress distribution in post in (1) models was more uniform when compared to (2) models. In all models the maximum concentration of S3 was found apically with the minimum value occurring right incisal to it except for model (2A) where the minimum S3 stress concentration occurs incisally. S3 stresses in post are much higher in (2) models when compared to (1) models. S3 stresses in post increased with decrease in bone level as shown in Figure 8.

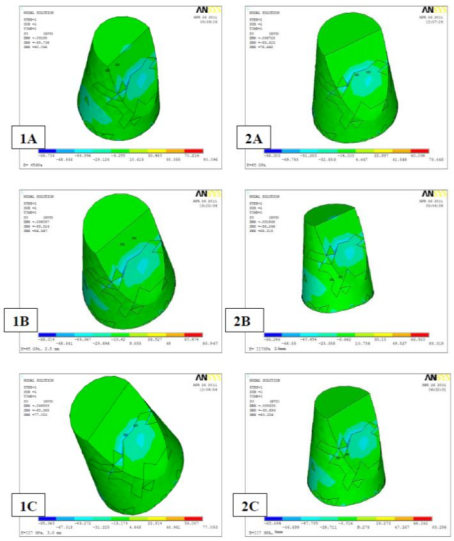

Figure 9: S_3 stress distribution in crown in different models under investigation.

Surprisingly, in crown, the order of S3 stresses distribution values when listed in a descending order are as follows; (1A), (2A), (1B), (2B), (1C), and (2C). Contour color plot analysis of the maximum third principle stress showed that stress distribution in crown in every model in group (1) was almost similar to its likewise in group (2).

In every model the S3 stress distribution was found to be almost uniform with maximum concentration located at area of load application for both models (2C) and (1C). In model (1A) it was located proximally and incisally while in model (2A) it was also located proximally but cervically. In model (1B) it was located lingually and incisally while in model (2B) it was located in the mid of proximal wall closer to the lingual side. values in models (1) are higher than in models (2) and are directly proportional to the bone level as shown in Figure 9.

On the other hand, in composite resin core , the order of S3 stress distribution values when listed in a descending order are as follows; (1A) (1B) (1C) (2A) (2B) (2C). Contour color plot analysis of the maximum third principle stress showed that stress distribution in core was almost similar in all models with the maximum values created lingually cervically and proximally extending facially. In (2) models the cervical lingual S3 stress concentration was extended too close to the proximal area of S3 high stress concentration. The lowest S3 values in core are found lingually incisally. The models in (1) group showed higher S3 values when compared to their likewise in (2) group. Values of S3 in composite resin core are found to be directly proportional to bone level.

- **Whole stress field distribution patterns (Von misses stress) (Seqv) (Table 6)**

Table 6: S_{eqv} (whole stress field) in Mega Pascal`s (MPa) of the components of the tested samples at different tested conditions:

Specimen \ Structure	Bone	Root	Post	Crown	Core
2A *Titanium post +2mm bone level*	134.832	41.777	26.494	152.719	10.498
2B *Titanium post +2.5mm bone level*	164.486	49.291	26.684	151.66	10.582
2C *Titanium post +3mm bone level*	181.354	68.115	30.616	150.487	10.726
1A *FRC post +2mm bone level*	135.47	41.249	15.838	156.628	9.213
1B *FRC post +2.5mm bone level*	165.289	48.717	15.974	155.779	9.247
1C *FRC post +3mm bone level*	182.402	67.487	16.117	155.116	9.308

Model (1C) showed highest value of Seqv in bone followed by models (2C), (2B), (1B), (2C) and (1C) respectively. By contour color plot analysis of the von misses stress distribution in bone it was found that Seqv stress is almost uniformly distributed in bone and was quite similar in all tested models. Maximum values of Seqv are found in inner aspect of bone cervically in all models. Values in (2) models are higher than their likewise in (1) models but still the difference was not significant. The Seqv values in bone are found to be directly proportional to bone loss.

When considering the root, it was found that model (2C) showed the highest value followed by (1C), (2B) and (1B) respectively. In the last place came both (1A) and (2A) with negligible difference between them. In all models, the maximum Seqv stress was located apically. Seqv stresses are high lingually, along the mid root extending cervically, while the minimum Seqv stress value was located facially cervically. The high Seqv stress located cervically decrease in area size with increase in bone loss. Seqv stress values in (2) models are insignificantly higher than in (1) models and are directly proportional to bone loss.

Seqv stress distribution in post in all tested models showed its highest value in both models (2A) and (2B) with almost no difference between them followed by model (2C). In third place came both models (1A) and (1B) with minute difference between them while in fourth place came model (1C). Contour color plot analysis of the von misses stress in post in all tested groups showed that maximum Seqv stress values are found incisally in all models except for model (2C) where it was located apically.

The minimum Seqv stresses values are found cervical to incisal

end of the post for all of the (1) models and in mid of body of the post in all of the (2) models. The Seqv values in (2) models are much higher than their likewise in (1) models and are directly proportional to bone loss .

Analyzing Seqv in crown in all studied models, it was found that model (1A) showed the highest value followed by both (1B) and (1C) with almost no difference between them. In third place came model (2C) followed by model (2B) and model (2A) respectively. Contour color plot analysis of the von misses stress showed that Seqv stress distribution in crown of all tested models was almost similar with highest values present lingually at site of load application. Values in (2) models are higher than those in (1) models and are inversely proportional to bone loss.

Studying Seqv stress distribution in composite resin core in studied models, it was found that models (2A,) (2B) and (2C) showed higher values when compared to models (1A), (1B) and (1C). The difference between all of the (2) models was minute which was the same for the (1) models.

Contour color plot analysis of the von misses stresses in composite resin core showed that Seqv stress distribution in core of all studied models was almost the same with the highest values found lingually incisally. Values found in (2) models are higher than those found in (1) models and are directly proportional to bone loss.

3.1.2 Displacement analysis:

Displacements occurring in different disassembled structures are identified and analyzed in the horizontal plane X (Ux). In the present study the X plane represents the buccal and lingual directions. Values of displacements are determined in Micro Meter (μm)

- **Displacement in X direction (Ux) (Table 7)**

Table 7: U_x (displacement in X direction) for the components of the tested samples at different tested conditions:

Structure / Specimen	Bone	Root	Post	Crown	Core
2A *Titanium post +2mm bone level*	0	0.002126	0.362E-03	-0.012959	-00.17564
2B *Titanium post +2mm bone level*	0.252E-04	0.002624	0.594E-03	-0.014767	-0.019941
2C *Titanium post +2mm bone level*	0.308E-03	0.003928	0.001143	-0.019736	-0.026119
1A *FRC +2mm bone level*	0	0.002097	0.360E-03	-0.012969	-0.017597
1B *FRC +2.5mm bone level*	0.164E-04	0.002593	0.594E-03	-0.014783	-0.019981
1C *FRC +2mm bone level*	0.299E-03	0.003895	0.001148	-0.01977	-0.026192

es in the tested models, it was found that in bone model (1A) showed no displacement at all. The highest value was found in model (2C) followed by models (1C), (2B), (1B)and (2A) respectively .

When considering the Ux in root in all models, the maximum value was found in model (2C) followed by models (1C) (2B) (1B) (2A) (1A) respectively .

Ux in post in model (1C) shows the highest value followed by models (2C), (1B), (2B), (1A) and (2A) respectively .

Model (1C) showed the highest Ux value, in crown, followed by model (2C), (1B), (2B), (1A) and (2A) respectively.

In composite resin core, the highest Ux was found in model (1C) followed by model (2C), (1B), (2B), (1A) and (2A) respectively .

4 Discussion and Conclusions

In dentistry, clinicians are usually faced by mutilated endodontically treated teeth requiring restoration. For reconstruction of teeth with substantial horizontal loss of the clinical crown, there is no realistic alternative to fabrication of post-core-crown complex. [**Error! Bookmark not defined.**,19] When tooth condition is complicated by bone loss, load capability of the tooth is decreased creating a higher incidence of restoration failure [20]. When bone support is reduced, the weak link becomes the tensile strength of the dentine which is dependent on the lever in addition to the presence of pre-existing flaws and the amount of remaining hard tissue, as a result, the fracture patterns change [**Error! Bookmark not defined.**-**Error! Bookmark not defined.**, **Error! Bookmark not defined.**-22]. For the long-term clinical success, the most critical task is to choose the correct post for each endodontically treated tooth which can resist the occlusal forces without failure such as root fracture, structural failure of the post itself or loss of retention. [23-29].

Everyday manufacturers supply new techniques and new materials of prefabricated posts and direct core build ups for better results. Multiple studies were carried out to compare the newly introduced post systems to one another and to old ones with proven clinical performance. Some studies used clinical testing for its realistic results in spite of its limitations due to human variation. Some of the earliest work used photo-elastic stress analysis techniques [**Error! Bookmark not defined.**]. To overcome the limitation of the previously mentioned techniques, studies used mechanical tests or computational evaluation of biomechanical responses of different structures of reconstructed teeth to loading (FEA) [**Error! Bookmark not defined.**].

The finite element analysis (FEA) is a well-known procedure for calculating stresses in a complex and irregular structures. Both Davy et al [**Error! Bookmark not defined.**] and Peters et al [**Error! Bookmark not defined.**] claimed that this computerized mathematical method has proven to be an extremely powerful analytical technique. In the present study, 3-D FEA was used to study the stresses in an idealized endodontically treated maxillary central incisor restored with post-core-crown complex. This was in accordance with many authors [**Error! Bookmark not defined.**-**Error! Bookmark not defined.**, **Error! Bookmark not defined.**, 22, **Error! Bookmark not defined.**, 31-39] who used 3-D models to obtain more realistic models and more accurate stress analysis. On the other hand, previous FEA investigations used 2-D models which were considered reliable when considering axial symmetric systems. Still spatial assessment of stresses and strains affecting a restorative system could not be correctly and precisely achieved as stated by Albuquerque et al, [**Error! Bookmark not defined.**] Reinhardt et al, [**Error! Bookmark not defined.**] Nakamura et al, [**Error! Bookmark not defined.**] Peters et al, [**Error! Bookmark not defined.**] Ukon et al, [40] and Pegoretti et al. [41]

In the present study non destructive sectioning using computerized tomography (CT) of an actual average sized maxillary central incisor was used. This was in accordance with Chen et al [**Error! Bookmark not defined.**] and Li-li et al [42]. Some researchers as Reinhardt et al, [**Error! Bookmark not defined.**] Lanza et al, [**Error! Bookmark not defined.**] Davy et al [**Error! Bookmark not defined.**] and Rodríguez-Cervantes et al [43] constructed their models using the average dimensions found in literature. Ricks-Williamson et al [44] used section images of actual dimensions after manual destructive slicing to obtain cross sections.

The first step was Multislice Computed Tomographic scanning (CT) of an average sized defect free central incisor obtaining a

serial of 2-D slices. This appeared to be the most accurate and realistic method to obtain the image required. Materialise's Interactive Medical Image Control System (MIMICS) computer software was used to generate a meshed 3-D central incisor model from the CT scan. Ansys 11 software was used to create all the 3-D models studied. Six 3–D finite element models of a rehabilitated root of upper central incisor were created. Three models were restored with fiber reinforced composite post while the remaining three were restored with titanium post. For each type of post, three different models were created, each with a different level of bone support; 2mm, 2.5mm, 3mm apical to the assigned cemento-enamel-junction C.E.J. For all tested models, periodontal ligament was created between root and bone to simulate more realistic clinical condition. This was in accordance with Toparli et al, [**Error! Bookmark not defined.**] Reinhardt et al [**Error! Bookmark not defined.**] Toksavul et al, [**Error! Bookmark not defined.**] Davy et al, [**Error! Bookmark not defined.**] Asmussen et al [34**Error! Bookmark not defined.**] and Rees. [45] Composite resin core and all metal nickel-chrome coping were created for all models with similar dimensions as in mechanical testing. Cement layers used to lute post and coping were also simulated. Similar to Peters et al [**Error! Bookmark not defined.**] post-cement interface was assumed to be perfectly bonded. 4 mm apical root canal filling was also created for all models in accordance to Toksavul et al [**Error! Bookmark not defined.**].

To obtain the stresses and displacements throughout the model, the elastic constants; E (modulus of elasticity) and (Poisson's ratio), were obtained from the literature and from manufacturers brochures and were assigned to the appropriate regions. Loading conditions were simulated on the created models in accordance to Peters et al [**Error! Bookmark not defined.**] while specification of elements was done in accordance with Davy et al [**Error! Bookmark not defined.**] by dividing the continuum to be analyzed into a set of discrete elements. These elements are connected with each other at nodes. [**Error! Bookmark not defined.**] Nods are identified at the corners of these elements or at additional points at the edges of the elements. [**Error! Bookmark not defined.**] A three dimensional co-ordinate system was used to define the locations of these nodes to specify the shape and size of the model. Nodal points were used to apply forces to the model. This was in accordance with Kishen et al. [**Error! Bookmark not defined.**] It was assumed that the load quantities are describable in terms of their values at the nodes. [**Error! Bookmark not defined.**] Similar to Kishen et al [**Error! Bookmark not defined.**] the displacements at the nodes were determined for the given loads, based on the initial boundary conditions and also the stress distribution and deformation were calculated from the nodal displacement using the stress-strain and strain-displacement relationship.

In the present study, by analyzing the contour color plots of the FEA results, it was found that the fiber reinforced composite posts served better when compared to titanium post. The maximum stresses were generally created in models rehabilitated with titanium post; maximum tensile stress was created in bone, internally, cervically and palataly. Followed by stresses created in crown, root, post and core respectively. Considering the maximum compressive stress, it was created also in bone cervically and internally but facially. Maximum Von Mises stresses were created in crown palataly followed by bone, root, post and core respectively.

These findings were in accordance with Chen et al, [**Error! Bookmark not defined.**] Asmussen et al, [34**Error! Bookmark not defined.**] Vasconcellos et al , [**Error! Bookmark not defined.**] and Pest et al [47] who compared stresses created in dentin when using titanium alloy and glass fiber reinforced composite posts. They found that the elastic modulus of post-core material affected the stress distribution pattern in dentine favoring the glass fiber reinforced composite post. Pegoritti et al [**Error! Bookmark not defined.**] found that using fiber reinforced post produced a stress field similar to that of natural tooth with lowest peak stresses inside the root except for some stress concentration cervically due to their high flexibility together with the less stiff core used. Rodríguez-Cervantes et al [**Error! Bookmark not defined.**] found that the glass fiber post induced a stress field quite similar to that of the natural tooth, with maximal stresses that did not vary with post or diameter length.

Unlike the previous findings, Toksavul et al [**Error! Bookmark not defined.**] found that in case both glass fiber reinforced and titanium posts stresses created in rehabilitated structures were minimal. Genovese et al [**Error! Bookmark not defined.**] found no significant difference in stresses created in rehabilitated models when either carbon fiber reinforced composite post was used or titanium post was used.

Considering the site of stress concentration, Toparli [**Error! Bookmark not defined.**] and Pegoritti et al [**Error! Bookmark not defined.**] claimed that the maximum stress values occurred at the cement metal post interface while Rodriguez-Cervantis et al [**Error! Bookmark not defined.**] found no stress concentration predicted along the fiber reinforced composite post juncture with core and dentine. Vasconcellos et al [**Error! Bookmark not defined.**] found two stress concentration regions; Adjacent to alveolar bone crest and dentine post boundary.

Toksavul et al [**Error! Bookmark not defined.**] found that the greatest stresses were found at the coronal third of the root on facial surfaces, regardless to the post type. Pegoritti et al [**Error! Bookmark not defined.**] found that the fiber reinforced post produced high stresses at the cervical region due to their high flexibility together with the less stiff core used. They also found that the glass fiber reinforced composite post produced a stress field similar to that of natural tooth. Kaur et al [48] found that all posts showed maximum stresses in the coronal and middle thirds of the root namely on the inner dentinal wall. Monzavi et al [32**Error! Bookmark not defined.**] found that stresses in dentine occurred in the coronal one third lingually on root while peak compressive stresses occurred facially on root. Santos et al [**Error! Bookmark not defined.**] found that the fiber post generated lower stresses along the interface and higher stresses in the root. Sorrentino et al [**Error! Bookmark not defined.**] found that, when fiber reinforced composite post was used, maximum stresses were recorded at the C.E.J. both buccally and palatally in both cementum and dentine while maximum strain values were recorded in middle third in buccal aspect of root surface. On the other hand, minimum values were recorded at level of both root apex and apical end of posts.

Nakamura et al [**Error! Bookmark not defined.**] found that when resin post is used less stresses are produced around the post tip when compared to metal ones.

In the present study, it was found that stresses in bone, root and post increased by decrease in bone level. Accordingly, the tendency of failure increased. Surprisingly, stresses decreased

by decrease in bone level in crown and the same was in core when considering tensile stresses only. This indicates the increase in stress concentration in root and bone thus increases the risk for their failure. Both compressive and von mises stresses in core did not change greatly by change in bone level. This might be explained by the fact that when bone resorbs, the support of the tooth diminishes with subsequent increase in lever action, as stated by Naumann et al, [**Error! Bookmark not defined.**] with subsequent descent in mechanical fulcrum together with the fracture resistance, as stated by Chen et al. [**Error! Bookmark not defined.**]

Similar to the findings of the present study, Reddy et al [49] and Reinhardt et al [**Error! Bookmark not defined.**] found that by decrease in bone level there was a significant increase in stresses apically. Moreover, Reinhardt et al [**Error! Bookmark not defined.**] found that the dramatically increasing stresses were concentrated in the little amount of dentine remaining at the post apex.

Under the testing conditions of the present study, the following concluded:

- For both tested posts with decrease simulated bone support concentration of tension stresses increased in root, post and bone but decreased in core and crown.
- For both post types stresses are more concentrated apically but with less stress values created in case of the tested fiber post thus decreasing the risk for root fracture.

REFERENCES

[1] G. Heydecke, F. Butz, A. Hussein and J. Strub," Fracture strength after dynamic loading of endodontically treated teeth restored with different post-and-core systems. J Prosthet Dent 2002; 87: 438-445.

[2] Willershausen B., Tekyatan H., Krummenauer F., Marroquin B.: Survival rate of endodontically treated teeth in relation to conservative vs post insertion techniques- A retrospective study. Eur J Med Res 2005; 10: 204-208.

[3] Duret B., Reynaud M. and Duret F..: New concept of coronoradicular reconstruction:the composipost. Chir Dent Fr 1990; 60: 131-141.

[4] Dallari A. and Rovatti L.: Six years of in vitro/in vivo experience with Composipost. Compend Contin Educ Dent Suppl 1996; 20: 57–63.

[5] Ferrari M., Vichi A., Mannocci F. and Mason P. Retrospective study of the clinical performance of fiber posts. Am J Dent 2000; 13: 9–13.

[6] Cormier C., Burns D. and Moon P.: In vitro comparison of the fracture resistance and failure mode of fiber, ceramic and conventional post systems at various stages of restoration. J Prosthodont 2001; 10: 1-26.

[7] Ottl P., Hahn L., Lauer H. and Fay M.: Fracture characteristics of carbon fiber, ceramic and non-palladium endodontic post systems at monotonously increasing loads. J Oral Rehab 2002; 29:175-183.

[8] Newman M., Yaman P., Dennison J., Rafter M. and Billy E.: Fracture resistance of endodontically treated teeth restored with composite posts. J Prosthet Dent 2003; 89:360-367.

[9] Chen X., Wu X., Niu L., Yang Y. and Yao W.: Effects of the loss of alveolar bone on the areas of periodontal ligament, mechanical fulcrum and fracture resistance of root and post-core system. Sichuan Da Xue Xue Bao Yi Xue Ban. (Abstract) (Article in Chinese)

[10] Plotino G., Grande N., Bedini R., Pameijer C. and Somma F.: Flexural properties of endodontic posts and human root dentin. J Dent Mat 2007; 23: 1129-1135.

[11] Ferrari M., Vichi A. and Garcia-Godoy F.: Clinical evaluation of fiber-reinforced epoxy resin posts and cast post and cores. Am J Dent 2000; 13: 15–18.

[12] Maccari P., Conceicao E. and Nunes M.: Fracture resistance of endodontically treated teeth restored with three different prefabricated esthetic posts. J Esthet Restor Dent 2003;15:25-30.

[13] Albuquerque R., Polleto L., Fontana R. and Cimini C.: Stress analysis of an upper central incisor restored with different posts. J Oral Rehab 2003; 30: 936–943.

[14] Toparli M.: Stress analysis in a post-restored tooth utilizing the finite element method. J Oral Rehab 2003; 30: 470–476.

[15] Reinhardt R., Krejci R., Pao Y. and Stannard J.: Dentin Stresses in Post-reconstructed Teeth with Diminishing Bone Support. J Dent Res 1983; 62: 1002-1008.

[16] Toksavul S, Zor M, Toman M, Gungor MA, Nergiz I and Artunc C.: Analysis of dentinal stress distribution of maxillary central incisors subjected to various post-and-core applications. J Oper Dent 2006; 31: 89-96.

[17] Lanza A., Aversa R., Rengo S., Apicella D. and Apicella A.: 3D FEA of cemented steel, glass and carbon posts in a maxillary incisor. J Dent Mat 2005; 21: 709–715.

[18] Davy D., Dilley G. and Krejci F.: Determination of Stress Patterns in Root-filled Teeth Incorporating Various Dowel Designs'. J Dent Res 1981; 60: 1301-1310.

[19] Qualtrough A., Chandler N. and Purton D.: A comparison of the retention of tooth-colored posts. Quint Int 2003; 34: 199-201.

[20] Sadeghi M.: A Comparison of the Fracture Resistance of Endodontically treated Teeth using Three Different Post Systems. J Dent 2006; 3: 69-75.

[21] Al-Omiri M. and Al-Wahadni A.: An ex vivo study of the effects of retained coronal dentine on the strength of teeth restored with composite core and different post and core systems. Int Endo J 2006; 39: 890-899.

[22] Dakshinamurthy S. and Nayar S. :The effect of post-core and ferrule on the fracture resistance of endodontically treated maxillary central incisors. Indian J Dent Res 2008; 19: 17-21.

[23] Gu X. and Kern M.: Fracture resistance of crowned incisors with different post systems and luting agents. J Oral Rehab 2002; 29:175-183.

[24] Al-Omiri M. and Al-Wahadni A.: An ex vivo study of the effects of retained coronal dentine on the strength of teeth restored with composite core and different post and core systems. Int Endo J 2006; 39: 890-899.

[25] Gu XH, Huang JP and Wang XX. An experimental study on fracture resistance of metal-ceramic crowned incisors with different post-core systems. Zhonghua Kou Qiang Yi Xue Za Zhi. 2007; 42: 169-72. (abstract) (article in Chinese)

[26] Duke E.: New directions for posts in restoring endodontically treated teeth. Compend Contin Educ Dent 2002; 23: 116-122.

[27] Nakamura T., Ohyama T., Waki T., Kinuta S., Wakabayashi K., Mutobe Y., Takano N. and Yatani H.: Stress analysis of endodontically treated anterior teeth restored with different types of post material. Dent Mater J 2006; 25: 145-50.

[28] Mannocci F., Ferrari M. and Watson T.: Intermittent loading of teeth restored using quartz fiber, carbon-quartz fiber, and zirconium dioxide ceramic root canal posts. J Adhes Dent 1991; 1: 153-158.

[29] Chen X., Li X., Guan Z., Liu X., Gu Y.: Effects of post material on stress distribution in dentine. Zhonghua Kou Qiang Yi Xue Za Zhi 2004; 39: 302-305. (Article in Chinese) (Abstract).

[30] Chalifoux P.: Restoration of endo ttt teeth: review, classification, and post design. Pract Periodont Aesthet Dent 1998; 10: 247-254.

[31] Saupe W., Gluskin A. and Radke R.: A comparative study of fracture resistance between morphologic dowel and cores and a resin-reinforced dowel system in the intraradicular restoration of structurally compromised roots. Quint Int 1996; 27: 483-91.

[32] Strub J., Pontius O. and Koutayas S.: Survival rate and fracture strength of incisors restored with different post and core systems after exposure in the artificial mouth. J Oral Rehab 2001; 28: 120-124.

[33] Rosentritt M., Sikora M., Behr M. and Handel G.: In vitro fracture resistance and marginal adaptation of metallic and tooth-colored post systems. J. Oral Rehab 2004; 31: 675-681.

[34] Naumann M., Preuss A. and Frankenberger R.: Reinforcement effect of adhesively luted fiber reinforced composite versus titanium posts. J Dent Mat 2007; 23: 138-144.

[35] Akkayan B. and Gülmez T.: Resistance to fracture of endodontically treated teeth restored with different post systems. J Prosthet Dent 2002; 87: 431-437.

[36] Desai S.: Principles and Technique of Using Bonded Post and Cores. Compend Contin Educ Dent 2006; 27: 439-445.

[37] Turker S., Alkumru H. and, Evren B.: Prospective clinical trial of polyethylene fiber ribbon-reinforced, resin composite post-core buildup restorations. Int J Prosthodont 2007 ; 20: 55-56.

[38] Mezzomo E., Massa F. and Libera S.: Fracture resistance of teeth restored with two different post and core designs cemented with two different cements: An in vitro study. Quint Int 2003; 34: 301-306.

[39] Grillages A.: Utilization of an esthetic post system for restoration of an endodontically treated tooth. Pract Periodont Aesthet Dent 1999; 11: 1087-1090.

[40] Turker S., Alkumru H. and, Evren B.: Prospective clinical trial of polyethylene fiber ribbon-reinforced, resin composite post-core buildup restorations. Int J Prosthodont 2007 ; 20: 55-56.

[41] Mezzomo E., Massa F. and Libera S.: Fracture resistance of teeth restored with two different post and core designs cemented with two different cements: An in vitro study. Quint Int 2003; 34: 301-306.

[42] Li-li L., Zhong-yi W., Zhong-cheng B., Yong M., Bo G., Hai-tao X., Bing Z. Zhang Y and Bing L.: Three-dimensional finite element analysis of weakened roots restored with different cements in combination with titanium alloy posts. Chinese Med J 2006; 119: 305-311.

[43] Rodríguez-Cervantes P., Sancho-Bru J., Barjau-Escribano A., Pérez-González A., and Forner-Navarro L.: Post Dimension Effect: Stress Distribution Pattern in Teeth Restored with Glass Fiber Prefabricated Posts . Proceedings. Biomech 2005; 9: 7-9.

[44] Grillages A.: Utilization of an esthetic post system for restoration of an endodontically treated tooth. Pract Periodont Aesthet Dent 1999; 11: 1087-1090.

[45] Torbjorner A., Karlsson S., Odman P.: Survival rate and failure characteristics for two post designs. J Prosthet Dent 1995; 73:439-444.

[46] Vasconcellos W., Cimini C. and Albuquerque R.: Effect of the post geometry and material on the stress distribution of restored upper central incisors using 3D finite element models. Stress distribution on incisors with posts. J Indian Prothodont Societ 2006; 6: 139-144.

[47] Trope M., Maltz D. and Tronstad L.: Resistance to fracture of restored endodontically treated teeth. Endod Dent Traumatol 1985;1:108-111.

[48] Pilo R., Cardash H., Levin E and Assif D.: Effect of core stiffness on the in vitro fracture of crowned, endodontically treated teeth. J Prosthet Dent 2002; 88: 302–30

[49] Peroz I., Blankenstein F., Lange K. and Naumann M.: Restoring endodontically treated teeth with posts and cores– a review. Quint Int 2005; 36: 737–746